

# Observations of Temperature and Frequency Dependence of AC Conductivity in Ytterbium Nitrate Crystal

R. Kawashima, R. Takahasi,<sup>1</sup> and H. Isoda

*Department of Materials Science and Engineering, Muroran Institute of Technology, Muroran 050, Japan*

Received April 10, 1995; in revised form June 27, 1995; accepted June 28, 1995

The ac conductivity of two samples of ytterbium nitrate crystal in the temperature range from  $-75$  to  $50^\circ\text{C}$  and in the frequency range from  $20$  to  $10^6$  Hz has been measured in several runs. We have observed metastable behavior of the conductivity in the region above  $-70^\circ\text{C}$ , and stable behavior below this temperature. The conductivity shows different frequency dependence in the metastable and the stable states. © 1996 Academic Press, Inc.

Rare earth nitrates,  $R(\text{NO}_3)_3 \cdot 6\text{H}_2\text{O}$ , in which  $R$  is a rare earth element, is a standard compound and the crystal symmetry is triclinic, with space group  $P\bar{1}$  at room temperature (1). Metastable phenomena, dependent on samples and measuring runs, have been found in electric measurements of the rare earth nitrate crystals (La (2), Nd (3), Sm (4), Eu (5), Gd (6), Tb (7) and Er (8) nitrates) at temperatures  $\sim 228 \text{ K} < T < \sim 283 \text{ K}$ .

Metastable magnetic behavior has been observed at temperatures in the range from  $4.2$  to  $300 \text{ K}$  in successive measurements on the gadolinium nitrate crystal using a SQUID detector system (9), (10). The aging effect of the electric properties has been observed in the crystals (La(2), Tb(11)). The chaotic properties of the phenomena have been given by the measurements and fractal analyses of the time series data of the electric behavior in samarium nitrate (12), (13).

However, the electric properties of ytterbium nitrate,  $\text{Yb}(\text{NO}_3)_3 \cdot 6\text{H}_2\text{O}$ , have been hitherto unknown (14). In the present paper, in order to study the electric properties of the ytterbium nitrate single crystal and the aging effect, the temperature and frequency dependencies of the ac conductivity along the  $c$ -axis have been measured at temperatures  $-75^\circ\text{C} \leq T \leq 50^\circ\text{C}$  and at frequencies  $20 \text{ Hz} \leq \nu \leq 1 \text{ MHz}$ . Data were collected in the heating and cooling runs for two samples.

<sup>1</sup> Present address: Hitachi Information & Control Systems, Inc., Katsuta 312, Japan.

## EXPERIMENTAL PROCEDURES

Experimental procedures and experimental apparatus have been given in a previous paper (6). Two specimens A and B were prepared from the different mother crystals at different aging period by cutting the crystal perpendicular to the  $c$ -axis.

Crystals used for the present measurements were grown in the same aqueous solution of ytterbium nitrate by decreasing the temperature. The mother crystal of sample A was grown from  $34.7^\circ\text{C}$  to  $33.7^\circ\text{C}$  for 1559 1-hour intervals; the mother crystal of sample B was grown from  $31.3^\circ\text{C}$  to  $30.0^\circ\text{C}$  for 480 1-hour intervals. These crystals were pure and of high quality. The clear crystal habit of the ytterbium nitrate crystal was similar to that of other rare earth nitrate crystals having six waters of crystallization.

Dimensions of samples A and B and aging conditions

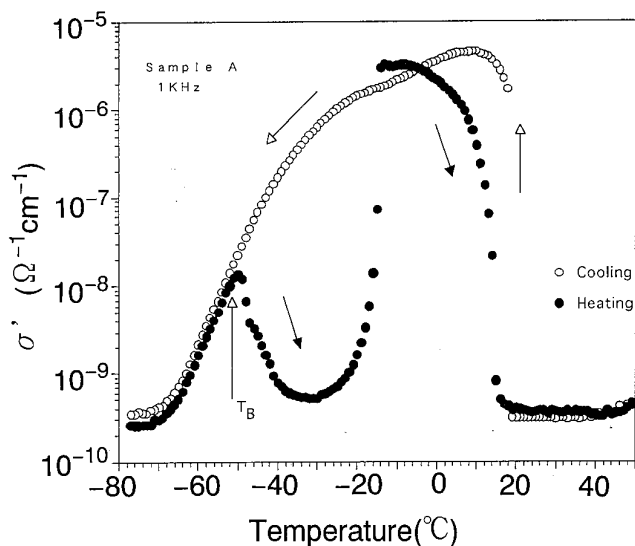


FIG. 1. The real part  $\sigma'$  of the complex conductivity  $\sigma^*$  at 1 kHz along the  $c$ -axis of an ytterbium nitrate crystal at temperatures  $T$  between  $50$  and  $-75^\circ\text{C}$  in the heating and cooling processes of the second run for sample A.

TABLE 1  
 Sizes of Two Samples, A and B, and Conditions of Measuring Runs  
 for the Respective Measurements

Sample name, Sample size area (cm <sup>2</sup> ), thickness (cm)	Number of measuring run	The measuring runs in temperature region	Aging periods (hours) from the crystal growth
A, 0.580 cm <sup>2</sup> , 0.203 cm	1	Cooling from 0°C to -75°C	28,920
		Heating from -75°C to 30°C	29,064
	2	Cooling from 50°C to -75°C	29,160
		Heating from -75°C to 50°C	29,304
	3	Cooling from 30°C to -75°C	36,792
		Heating from -75°C to 40°C	36,912
	4	Cooling from 41°C to -75°C	37,008
		Heating from -75°C to 30°C	37,128
	5	Cooling from 30°C to -75°C	37,920
		Heating from -75°C to 20°C	38,016
	6	Cooling from 20°C to -75°C	38,112
		Heating from -75°C to 20°C	38,232
	7	Cooling from 20°C to -75°C	38,352
		Heating from -75°C to 20°C	38,472
B, 0.386 cm <sup>2</sup> , 0.090 cm	1	Cooling from 20°C to -75°C	168
		Heating from -75°C to 20°C	264
	2	Cooling from 20°C to -75°C	384
		Heating from -75°C to 20°C	504
	3	Cooling from 20°C to -75°C	624
		Heating from -75°C to 20°C	732
	4	Cooling from 20°C to -75°C	852
		Heating from -75°C to 20°C	960
	5	Cooling from 20°C to -75°C	1056
		Heating from -75°C to 20°C	1164
	6	Cooling from 20°C to -75°C	1272
		Heating from -75°C to 20°C	1392
	7	Cooling from 20°C to -75°C	1500
		Heating from -75°C to 20°C	1608
	8	Cooling from 20°C to -75°C	1716
		Heating from -75°C to 20°C	1824
	9	Cooling from 20°C to -75°C	1932
		Heating from -75°C to 20°C	2040

*Note.* The aging period is defined as the time elapsed after the mother crystal was grown.

are given in Table 1. The cut surfaces of the samples were polished. The contact electrodes used in the measurements were made with silver paste (Tokuriki Chem. Inst. P255). The good qualities of the electrodes and the specimens have been retained at the final stage of the experiment.

The electrical conductivity spectrum of the crystal in the frequency range from 20 Hz to 1 MHz and at temperatures in the region from 50°C to -75°C was measured automatically by an LCR meter (HP4284A) controlled by a computer (NEC PC9801E) through the general purpose interface bus (GPIB). The schematic diagram of the experimental apparatus is given in Ref. (12), as the scheme is partially different from that used in the present study.

The specimen was mounted in a massive copper block, of weight 10 kg, and submerged in a silicon oil bath, which

is used to avoid decomposition of the sample and evaporation of the water of crystallization and to maintain thermal homogeneity. The variation in the chemical state of the specimens has not been observed at the final stage in the process of the measuring runs. The copper block is set in an adiabatic stainless steel holder surrounded by alcohol, kept at -80°C by cooler (Tokyo Rikakikai Co.LTD., EC-80). The temperature of the specimen was measured with a copper-constantan thermocouple mounted in the sample cell and stabilized to within  $\pm 0.1^\circ\text{C}$  in the subsequent measuring runs, controlled by the computer.

## RESULTS AND DISCUSSION

The real part  $\sigma'$  of the complex conductivities  $\sigma^*$  along the *c*-axis of the crystal at 1 kHz is shown in Fig. 1 at

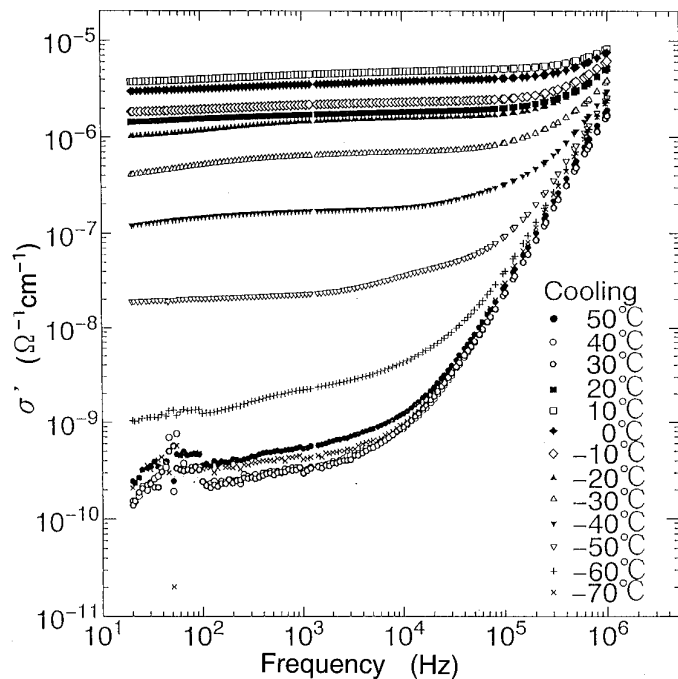


FIG. 2. Frequency variation of the real part  $\sigma'$  for the complex conductivity  $\sigma^*$  at several temperatures in the cooling process of the second run for sample A.

temperatures  $T$  between 50 and  $-75^\circ\text{C}$  in the cooling and heating processes of the second run for sample A. The results are given as a typical example of  $\sigma'(T)$  observed in the measurements given in Table 1.

As seen in Fig. 1,  $\sigma'(T)$  shows temperature dependence

with thermal hysteresis in the region between 20 and  $-70^\circ\text{C}$  for the cooling and heating process. Bifurcated behavior in the temperature variation of  $\sigma'(T)$  has been found near  $-50^\circ\text{C}$  in the cooling and the heating processes. The bifurcation point is defined by the arrow  $T_B$  in Fig. 1. The temperature range in which the behavior of  $\sigma'(T)$  is observed in the ytterbium nitrate crystal is larger than those of  $\sigma'(T)$  found in other rare earth nitrates. The bifurcation phenomenon is a new one found in the crystal.

Figure 2 shows the frequency dependence of  $\sigma'$  on the logarithmic plane in the range  $20 \text{ Hz} \leq \nu \leq 1 \text{ MHz}$  at several temperatures for the cooling process of the second run for sample A. The conductivity  $\sigma'$  in Fig. 2 may be represented by the relation  $\sigma'(\nu, T) = A\nu^s$ , where  $s$  is the frequency exponent. The value of  $s$ , derived from the frequency gradient of  $\sigma'(\nu)$  in the range from 30 kHz to 1 MHz, is  $0 < s < 1$  for temperatures in the region  $-50^\circ\text{C} < T < 10^\circ\text{C}$ , within which the temperature dependence of the conductivity has been observed. The behavior of  $\sigma'$  in the ytterbium nitrate crystal is similar to that in other rare earth nitrates.

The temperature dependence of the real part  $\sigma'$  of the complex electric conductivity  $\sigma^*$  at 1 kHz is given in Figs. 3 and 4 for several measuring runs in both heating and cooling processes from  $50^\circ\text{C}$  to  $-75^\circ\text{C}$  for the samples A and B, respectively. Experimental conditions of the measuring runs are given in Table 1.

As shown in these figures, results given in the measuring runs of the initial stage show appreciable temperature variation of  $\sigma'$  with thermal hysteresis in the region from  $20^\circ\text{C}$  to  $\sim -70^\circ\text{C}$ . In the subsequent measuring runs, however,

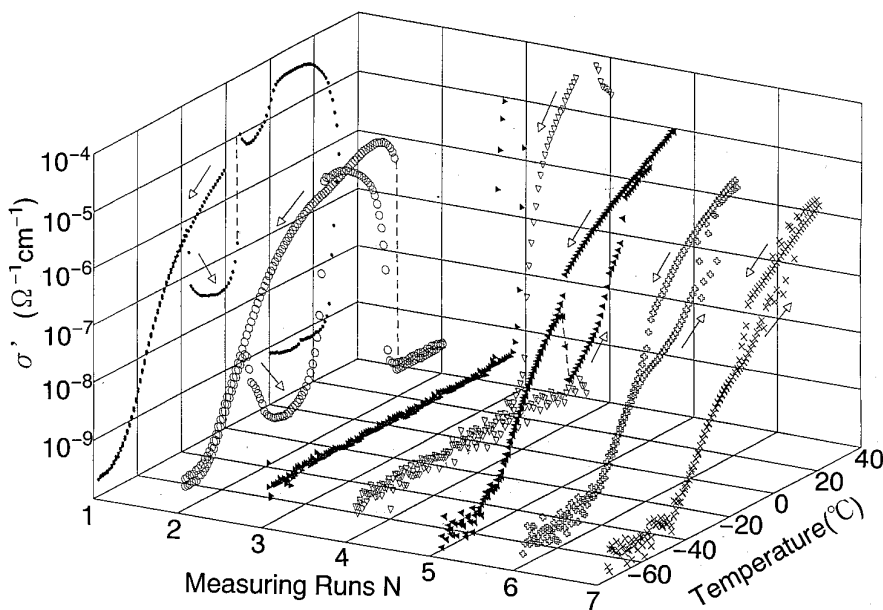


FIG. 3. Temperature dependence of the real part  $\sigma'$  of the complex conductivity  $\sigma^*$  of an ytterbium nitrate crystal along the  $c$ -axis in the heating and cooling runs at 1 kHz for sample A.

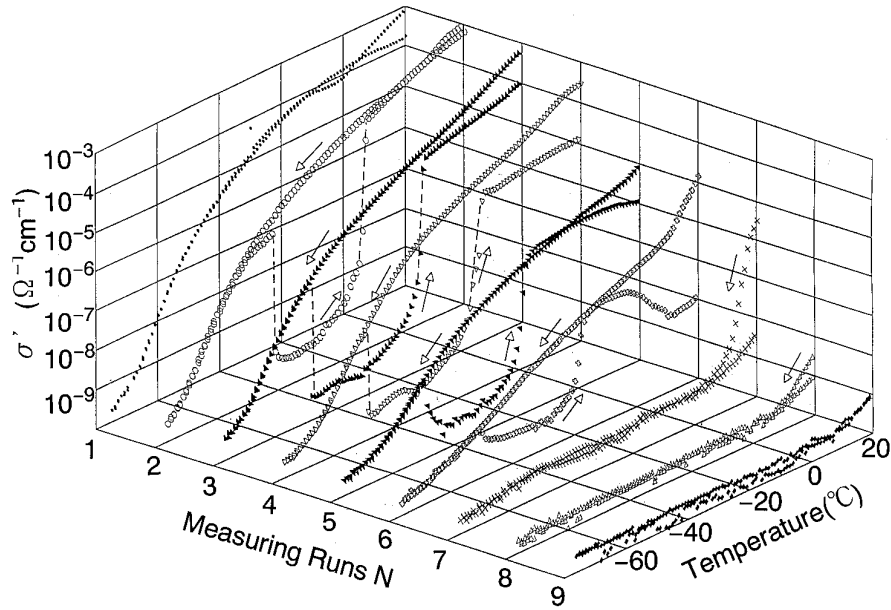


FIG. 4. Temperature dependence of the real part  $\sigma'$  of the complex conductivity  $\sigma^*$  of an ytterbium nitrate crystal along the  $c$ -axis in the heating and cooling runs at 1 kHz for sample B.

similar behaviors were not observed in the temperature range.

To define the dependence of  $\sigma'$  on the subsequent measuring runs, in Figure 5, values of  $\sigma'$  at 20 and  $-75^{\circ}\text{C}$  are plotted as a function of measuring runs for two samples.

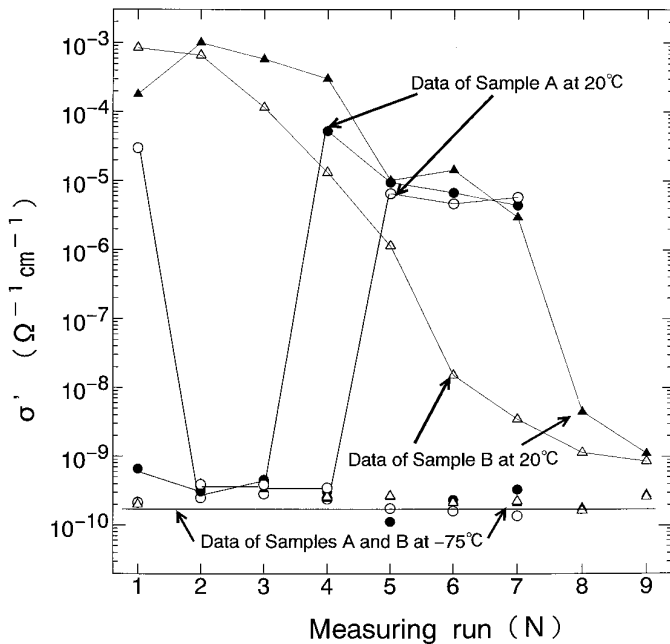


FIG. 5. The dependence of  $\sigma'$  at 20 and  $-75^{\circ}\text{C}$  on the subsequent measuring runs for the samples A and B; heating ( $\circ$ ) and cooling ( $\bullet$ ) for the sample A; heating ( $\Delta$ ) and cooling ( $\blacktriangle$ ) for the sample B.

Values of  $\sigma'$  at  $-75^{\circ}\text{C}$  are nearly constant at  $10^{-10}\ \Omega^{-1}\text{cm}^{-1}$ , with dispersion of data in the subsequent measuring runs. On the other hand, as shown in Fig. 5, values of  $\sigma'$  at  $20^{\circ}\text{C}$  have changed from  $10^{-3}\ \Omega^{-1}\text{cm}^{-1}$  to  $10^{-9}\ \Omega^{-1}\text{cm}^{-1}$  in the measuring process. In our present experimental study of the ytterbium nitrate crystal, the behavior given in Fig. 5 has been irreversible during the measuring runs 1 and 9. The phenomena correspond to an irreversible aging pro-

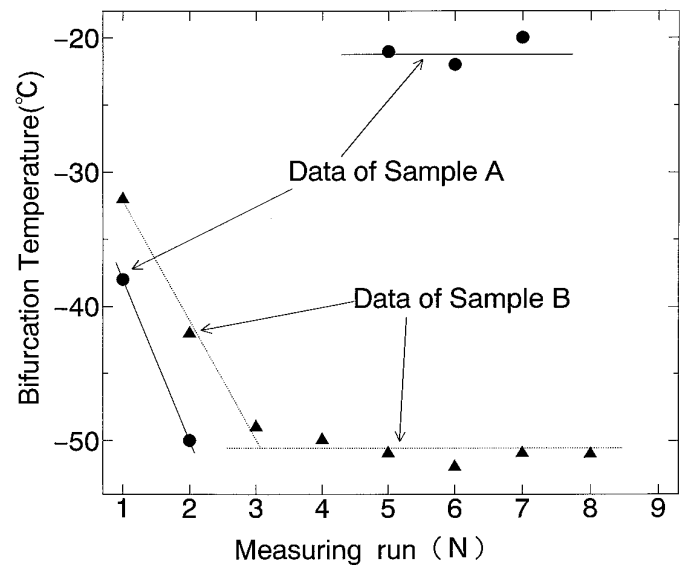


FIG. 6. The dependence of bifurcation temperature  $T_B$  in the functional form of  $\sigma'(T)$  on the subsequent measuring runs for the samples A and B.

cess from a metastable state to a stable one or to a structural relaxation process (15) which has been found in other rare earth nitrate crystals (La and Tb) (2), (11).

The dependence of the bifurcation temperature on the measuring runs is shown in Fig. 6 for the samples to define the effect of aging on the bifurcation phenomena given in Fig. 1. The value of  $T_B$  in Fig. 6 appears constant in the later measuring run as the response of the crystal shows a transition from the metastable to the stable state. This observation is similar to the bifurcation point crossing the boundary separating the stable and unstable solutions of the nonlinear differential equation to represent dynamics of nonlinear and nonequilibrium systems (16).

In the present study, we have found the characteristic electrical properties of the ytterbium nitrate crystal. The origin of the phenomena would be related to the nonlinear dynamics of a rare earth ion caged in a polyhedron having high coordination linked with the hydrogen network (17). However, in order to understand the microscopic structure of the phenomena, it is necessary to observe the microscopic properties in detail, such as structural configuration or electronic energy levels of the rare earth ions in the rare earth nitrate crystals, by using methods of structural analyses or optical measurements.

## REFERENCES

1. K. A. Gshneider Jr. and L. Eyring, Eds., "Handbook on the Physics and Chemistry of Rare Earths," Vol. 8, pp. 302–334. North-Holland, Amsterdam, 1986.
2. R. Kawashima, T. Saitoh, and H. Isoda, *J. Phys. Soc. Jpn.* **62**, 4529 (1993).
3. R. Kawashima and M. Hattori, *J. Phys. Soc. Jpn.* **61**, 1427 (1992).
4. R. Kawashima and Y. Matsuda, *J. Phys. Soc. Jpn.* **59**, 3727 (1990).
5. R. Kawashima, *Solid State Commun.* **78**, 553 (1991).
6. R. Kawashima and H. Isoda, *J. Phys. Soc. Jpn.* **59**, 3408 (1990).
7. R. Kawashima, S. Nasukawa, and H. Isoda, *J. Solid State Chem.* **107**, 503 (1993).
8. R. Kawashima, *J. Phys. Soc. Jpn.* **60**, 342 (1991).
9. R. Kawashima and H. Isoda, *Phys. Stat. Sol. (a)* **145**, K59 (1994).
10. R. Kawashima and H. Isoda, *J. Phys. Soc. Jpn.* **64**, 684 (1995).
11. R. Kawashima, S. Nasukawa, and H. Isoda, *J. Phys. Soc. Jpn.* **64**, 1439 (1995).
12. R. Kawashima, S. Nishimura, and H. Isoda, *Physica B* **183**, 135 (1993).
13. R. Kawashima, S. Nishimura, and H. Isoda, *Physica B* **203**, 59 (1994).
14. "Gmelin Handbuch der Anorganischen Chemie," System – number 39. Springer-Verlag, Berlin/New York, 1974.
15. K. Kawasaki *et al.*, Eds., "Slow dynamics in Condensed Matter." Amer. Insti. of Phys., New York, 1991.
16. P. Berge, Y. Pomeau, and C. Vidal, "Order within Chaos." Wiley, New York, 1984.
17. E. L. Muettertics and C. M. Wright, *Q. Rev. Chem. Soc.* **21**, 109 (1967).